Arch. Pharm. Chem. Life Sci. 2016, *349*, 293–301

ARCH PHARM
Archiv der Pharmazie

Full Paper

Phthalimide-Derived *N*-Benzylpyridinium Halides Targeting Cholinesterases: Synthesis and Bioactivity of New Potential Anti-Alzheimer's Disease Agents

Mina Saeedi[1,2], Maedeh Golipoor[3], Mohammad Mahdavi[4], Alireza Moradi[5], Hamid Nadri[5], Saeed Emami[6], Alireza Foroumadi[3], and Abbas Shafiee[3]

[1] Medicinal Plants Research Center, Faculty of Pharmacy, Tehran University of Medical Sciences, Tehran, Iran
[2] Persian Medicine and Pharmacy Research Center, Tehran University of Medical Sciences, Tehran, Iran
[3] Department of Medicinal Chemistry, Faculty of Pharmacy and Pharmaceutical Sciences Research Center, Tehran University of Medical Sciences, Tehran, Iran
[4] Drug Design and Development Research Center, Tehran University of Medical Sciences, Tehran, Iran
[5] Faculty of Pharmacy, Department of Medicinal Chemistry, Shahid Sadoughi University of Medical Sciences, Yazd, Iran
[6] Faculty of Pharmacy, Department of Medicinal Chemistry and Pharmaceutical Sciences Research Center, Mazandaran University of Medical Sciences, Sari, Iran

In order to develop potent dual-binding cholinesterase inhibitors as potential drugs for the treatment of Alzheimer's disease, we designed and synthesized phthalimide-based acetylcholinesterase (AChE) inhibitors (**7**) containing a substituted *N*-benzylpyridinium residue. The *in vitro* anti-cholinesterase assay employing the target compounds against AChE and butyrylcholinesterase (BChE) revealed the 2-fluorobenzylpyridinium derivative **7d** as the most potent compound against both enzymes, with IC_{50} values of 0.77 and 8.71 μM. The docking study of compound **7d** into the active site of AChE showed the gorge-spanning binding mode, in which the compound spans the narrow hydrophobic gorge from the bottom to the rim.

Keywords: 1,3-Dioxoisoindoline / Acetylcholinesterase / Alzheimer's disease / Phthalimide / Pyridinium

Received: November 25, 2015; Revised: January 28, 2016; Accepted: February 1, 2016

DOI 10.1002/ardp.201500425

Additional supporting information may be found in the online version of this article at the publisher's web-site.

Introduction

Alzheimer's disease (AD) is an age-related neurodegenerative disease that affects more than 30 million people around the world [1]. AD is characterized by the main symptoms of progressive memory loss, cognition defect, and behavioral impairment, which consequently leads to the disability and death. This situation intensely influences the patient's social life and activity [2, 3].

The main pathophysiological feature of AD is a significant deficit in cholinergic transmission due to damage to cholinergic neurons in certain parts of the brain [4, 5]. Accordingly, one of the effective strategies to relieve the AD symptoms is increasing the acetylcholine (ACh) level in the brain through the inhibition of acetylcholinesterase (AChE). The inhibition of AChE may restore the cholinergic function in the brain and significantly reduce the severity of AD [6, 7]. The obtained results from clinical trial studies indicated that AChE inhibitors such as donepezil, galantamine, or rivastigmine improve cognitive function in patients with AD [8, 9].

Correspondence: Dr. Abbas Shafiee, Faculty of Pharmacy and Pharmaceutical Sciences Research Center, Department of Medicinal Chemistry, Tehran University of Medical Sciences, Tehran 14176-14411, Iran.
E-mail: ashafiee@ams.ac.ir
Fax: +98 21 66461178

Furthermore, several evidences suggest that inhibition of butyrylcholinesterase (BChE) in the brain would be an important therapeutic target for AD therapy since BChE is an important co-regulator of cholinergic neurotransmission [10, 11]. Also, numerous findings have shown that AChE and BChE have additional non-catalytic properties such as proteins' activity modulation and amyloid cascade inhibition [9, 12–15]. Hence, both AChE and BChE inhibitors are supposed to have great potential in the AD therapy.

Based on X-ray crystallographic studies, the structure of AChE consists of two active centers: the catalytic anionic site (CAS) located at the bottom of a deep narrow gorge – with the AChE catalytic triad and the anionic subsite, and the peripheral anionic site (PAS) near the entrance of the gorge [16, 17]. It was demonstrated that dual-binding AChE inhibitors – that interact with CAS and PAS, were more potent inhibitors compared to the ligands that interact with only one site of the enzyme [18–20].

Accordingly, many efforts have been made to develop potent dual-binding AChE inhibitors as potential drugs for treatment of AD. Among them, donepezil analogs (Fig. 1) have been studied more extensively. The experimental and computational studies on the binding interactions of donepezil with AChE indicated that the *N*-benzylpiperidine moiety of the molecule interacts with the CAS, while the indanone part binds to the PAS [21, 22].

Previously, we have designed coumaranone-based AChE inhibitors (Fig. 1) containing the *N*-benzylpyridinium moiety as dual-binding agents in which the *N*-benzylpyridinium part of the molecules interacts with the CAS and the aromatic part of coumaranone ring engages in π–π stacking interaction with the aromatic amino acid residues in the PAS [23]. It should be noted that the pyridinium-type AChE inhibitors have received much attention as multi-potent AD modifying agents [24]. In continuation of our work on pyridinium-type compounds targeting cholinesterases [23–27], we considered the phthalimide scaffold as a PAS binder for the AChE enzyme. The phthalimide scaffold was reported to interact with the PAS of AChE instead of the indanone fragment of donepezil [28–30]. Furthermore, several AChE inhibitors were designed based on the phthalimide pharmacophore [31–34]. Therefore, in continuation of our efforts on the synthesis of bioactive compounds [35–39], herein we report synthesis, *in vitro* biological evaluation, and docking study of *N*-benzylpyridinium-type compounds **7** bearing phthalimide scaffolds. The type and position of substituent on the *N*-benzyl residue were modified for structure–activity relationships (SAR) study. Furthermore, a limited series of succinimide derivatives **8** was prepared and evaluated to prove the importance of the aromatic part of the molecules **7** (Fig. 1).

Results and discussion

Chemistry

The synthetic routes to target compounds **7** and **8** were illustrated in Scheme 1. The reaction of phthalimide (**1**) or succinimide (**2**) with 4-(bromomethyl)pyridine (**3**) in the presence of K_2CO_3 in DMF afforded intermediates **4** or **5**. Subsequent *N*-benzylation of pyridine derivatives **4** or **5** using various benzyl halides **6** gave the corresponding *N*-benzylpyridinium salts **7** or **8**.

Cholinesterase inhibition activity

The phthalimide and succinimide derivatives **7a–m** and **8a–c** were evaluated for their *in vitro* cholinesterase activity against AChE and BChE. The IC_{50} values of the test compounds in comparison to standard drug donepezil are presented in Table 1. As can be seen in Table 1, all compounds showed excellent to mild inhibitory activity (IC_{50} values = 0.77–22.12 μM) toward AChE. The 2-fluorobenzyl derivative **7d** with IC_{50} value of 0.77 μM was the most potent compound against AChE. Its activity was fivefold more than that of unsubstituted benzyl analog **7a**. Similarly, the 2-bromobenzyl analog **7k** was more potent than compound **7a**. Thus, the

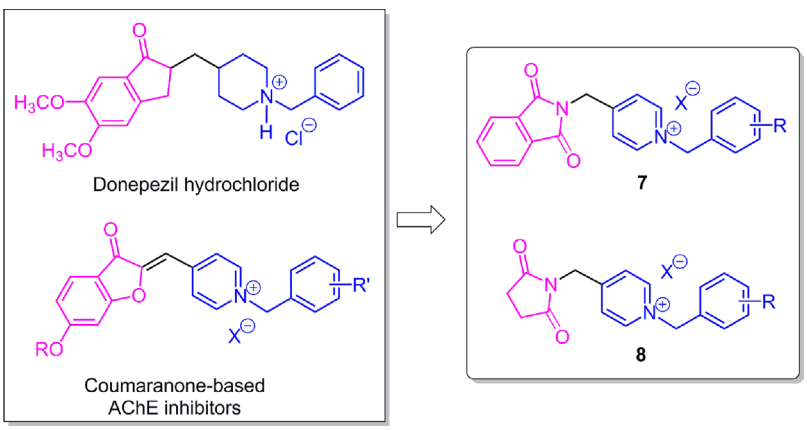

Figure 1. Design of target compounds phthalimide-derived benzylpyridinium halides **7** and related succinimide derivatives **8**.

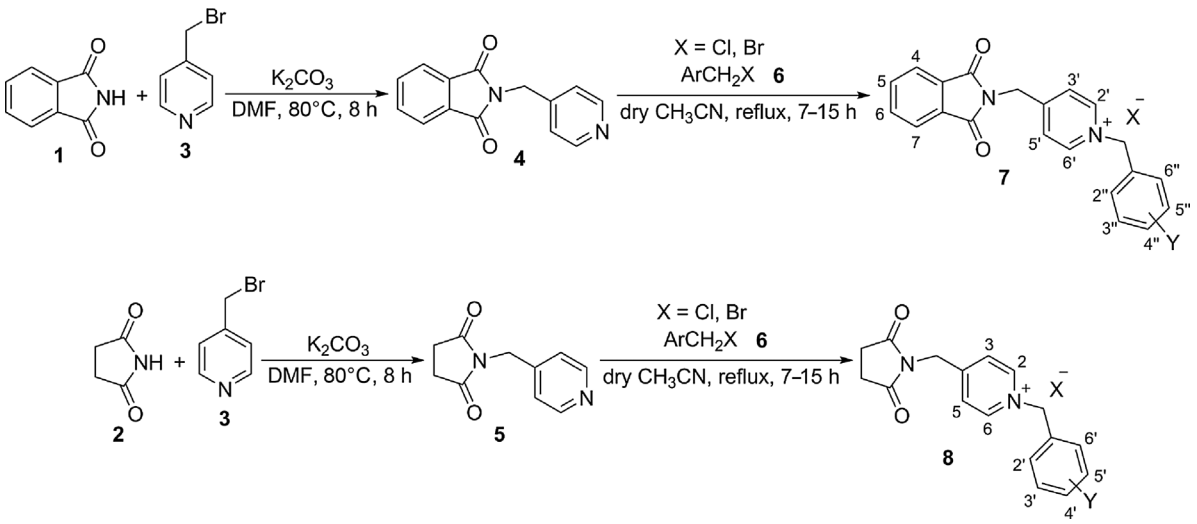

Scheme 1. Synthesis of phthalimide/succinimide-derived benzylpyridinium halides **7** or **8**.

introduction of 2-flouro or 2-bromo substituent on benzyl moiety improved the anti-AChE. In contrast, substitution of halogen at the positions 3 and 4 had negative effect on inhibitory potency against AChE. Among the dichloro derivatives, the 2,6-dichloro analog **7h** showed better activity to inhibit AChE. The decreased activity in the compound bearing a *meta*- or *para*-substituent may be due to the steric effect in these positions.

4-Fluoro, 3-fluoro, and 2,3,5-trifluoro derivatives (compounds **7b**, **7c**, and **7e**, respectively) showed equal inhibitory activity against AChE. Comparison of fluorobenzyl derivatives with their corresponding bromobenzyl analogs revealed that fluoro group was better than bromo group. Also, the introduction of nitro substituent as a strong electron-withdrawing group into position 2 or 4 could not improve the activity.

The obtained results from the limited series of succinimide derivatives **8a–c** demonstrated that the replacement of phthalimide with succinimide diminished the anti-AChE activity. This finding indicates that the aromatic part fused to the succinimide scaffold has important role in the inhibitory activity of the designed molecules. In contrast to the phthalimide series, the introduction of 3-fluoro substituent on the benzyl group in succinimide series could improve the anti-cholinesterase activity.

Table 1. Inhibitory activities (IC_{50}, μM) of compounds 7a–m and 8a–c against AChE and BChE.

Compound	X	R	AChE	BChE
7a	Br	H	4.29 ± 0.13	20.07 ± 0.11
7b	Cl	4-F	6.90 ± 0.2	84.87 ± 0.13
7c	Cl	3-F	6.14 ± 0.05	50.56 ± 0.20
7d	Cl	2-F	0.77 ± 0.17	8.71 ± 0.18
7e	Cl	2,3,5-F_3	6.77 ± 0.17	67.02 ± 0.21
7f	Cl	2,4-Cl_2	21.00 ± 0.20	>100
7g	Cl	3,4-Cl_2	13.8 ± 0.11	78.52 ± 0.11
7h	Cl	2,6-Cl_2	5.81 ± 0.10	61.23 ± 0.18
7i	Br	4-Br	9.34 ± 0.17	81.25 ± 0.22
7j	Br	3-Br	11.35 ± 0.14	60.83 ± 0.20
7k	Br	2-Br	2.16 ± 0.11	15.65 ± 0.22
7l	Br	4-NO_2	11.23 ± 0.15	>100
7m	Br	2-NO_2	9.28 ± 0.11	>100
8a	Br	H	18.3 ± 0.18	>100
8b	Br	3-F	7.19 ± 0.21	45.61 ± 0.13
8c	Br	3-Br	22.12 ± 0.11	50.10 ± 0.11
Donepezil			0.023 ± 0.01	0.35 ± 0.02

ARCH PHARM
Archiv der Pharmazie

The IC_{50} values of compounds against AChE and BChE indicated that the inhibitory activity of all compounds against BChE was significantly less than AChE. Compounds **7f**, **7l**, **7m**, and **8a** showed no activity against BChE (IC_{50} values $> 100\,\mu M$). However, the most potent compound against AChE (compound **7d**) showed also the highest activity against BChE ($IC_{50} = 8.71\,\mu M$). The obtained IC_{50} value for unsubstituted compound **7a** was $20.07\,\mu M$. The introduction of 2-fluoro or 2-bromo substituents into phthalimide derivatives could increase the anti-BChE activity (for example, compounds **7d** and **7k**), but other substituents diminished the activity toward BChE. Meanwhile, the presence of 3-fluoro and 3-bromo groups in the succinimide analogs had positive effect for anti-BChE activity.

Kinetic study of AChE inhibition

For exploring the inhibition mechanism of designed compounds, the kinetics of AChE inhibitory activity by the most potent compound **7d** was studied. The rate of the enzyme catalysis was measured at three different concentrations of the inhibitor (0.4, 0.8, $1.6\,\mu M$) and the substrate (0.14, 0.33, and $0.70\,\mu M$ of acetylthiocholine iodide). The constructed Lineweaver–Burk plot (Fig. 2) revealed that both slopes and intercepts increased by rising the inhibitor concentrations. This pattern suggested the mixed-type of inhibition by compound **7d**. Also, the secondary plot (Fig. 3) was used to predict the K_i value. The obtained K_i value of compound **7d** was $1.81\,\mu M$.

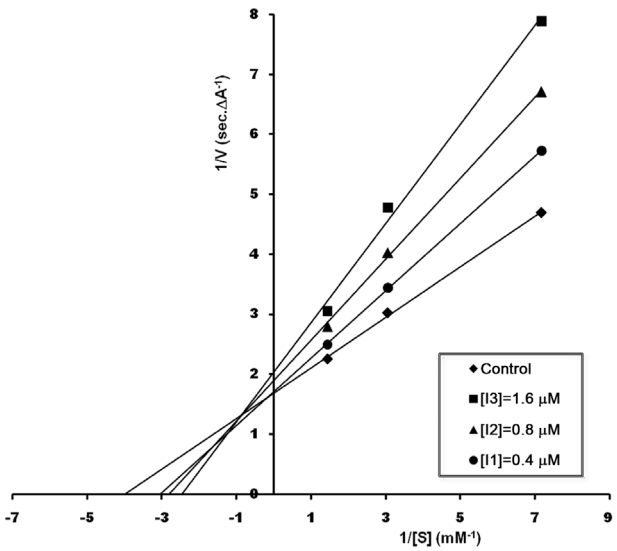

Figure 2. Overlaid Lineweaver–Burk reciprocal plot of AChE initial velocity at increasing substrate concentrations using different concentrations of compound **7d**.

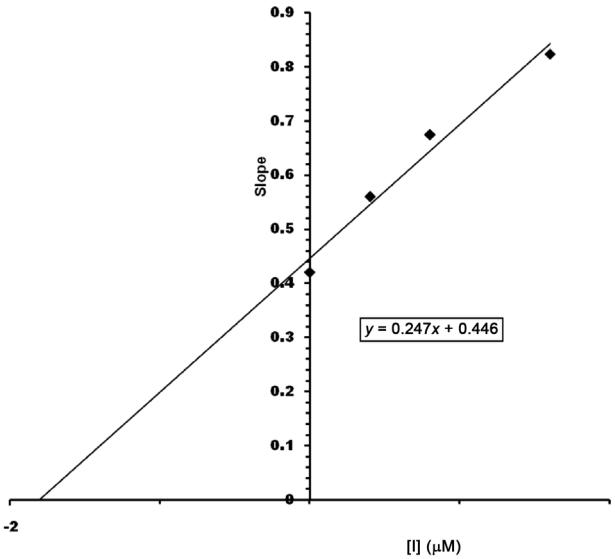

Figure 3. A secondary plot of Lineweaver–Burk plot versus inhibitor (compound **7d**) concentration.

Molecular docking study

In order to understand the mode of interaction between this new class of inhibitors and AChE, the most active compound **7d** was docked as a representative member of title compounds (Fig. 4). To validate the applied docking protocol, the native ligand, donepezil, was redocked into the binding site of the enzyme. The root mean square deviation (RMSD) of the redocked and native ligand pose was 0.85 Å (Fig. 5), indicating the capability of the protocol for the valid docking of this ligand–receptor complex system.

The three-dimensional structure of **7d** was sketched and then energy minimized using HyperChem 7 (Hypercube, Inc.) by the following parameters: a distance gradient algorithm with convergence criterion of 0.05 kcal/(mol Å) and a maximum of 1000 iterations. Molecular docking was carried out using Autodock 4.0 [40]. AChE co-crystalized with *N*-saccharinohexyl-galanthamine (PDB id; 3I6Z) was used as a receptor. The geometric center of the ligand was used to define the active site interactions points. The docking result was further analyzed by Accelrys Discovery Studio Visualizer 3.0 (Accelrys Software Inc., San Diego). The best pose of docking was selected in terms of free energy of binding. As shown in Fig. 4, the inhibitor was anchored in the mid-gorge recognition site by making a cation–π interaction with Phe329. In this way, the benzyl moiety was stacked toward Trp83. This orientation allowed formation of hydrogen bond between 2-fluoro group and Glu199. The phthalimide part of the molecule also contributed in making a hydrogen bond with Tyr120. Particularly, two aromatic-hydrophobic patches of the active site namely CAS (catalytic anionic subsite) and PAS (anionic site) or mid-gorge recognition site were involved in the interactions. As seen in Fig. 4, compound **7d** showed gorge-

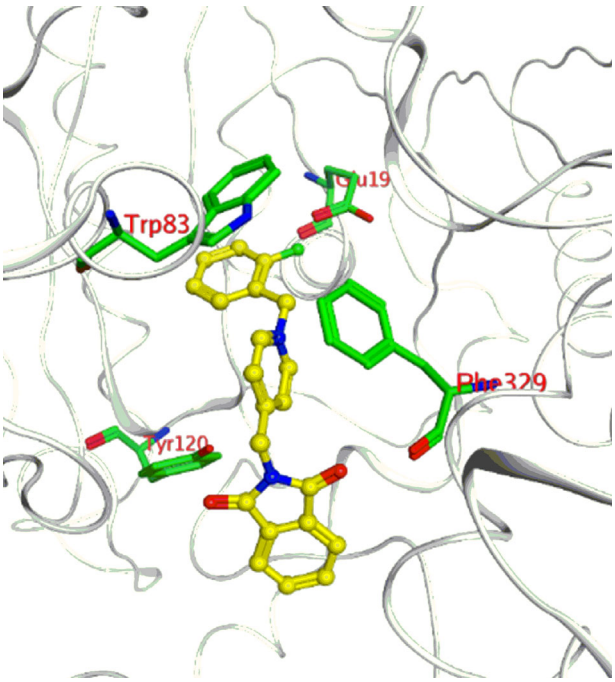

Figure 4. Selected residues of the protein binding site of AChE in complex with compound **7d**.

spanning binding mode in which the compound spans the narrow hydrophobic gorge from the bottom to the rim.

Furthermore, to elucidate the mode of interaction between compound **7d** and BChE, the same protocol was used (Fig. 6). Human butyrylcholinesterase (PDB code: 4TPK) was used as a target for docking and Trp82 was selected as binding center. Molecular docking studies demonstrated that compound **7d** was well accommodated inside the binding pocket of BChE. The best selected dock pose of **7d** exhibited a π–π interaction with Trp82 by participation of phthalimide moiety (Fig. 6). Moreover, the pendant fluorobenzyl moiety depicted hydrophobic interactions with Trp231 and Phe329. Also, a F–π interaction assisted compound **7d** to attain a favorable orientation toward the binding residue Trp231.

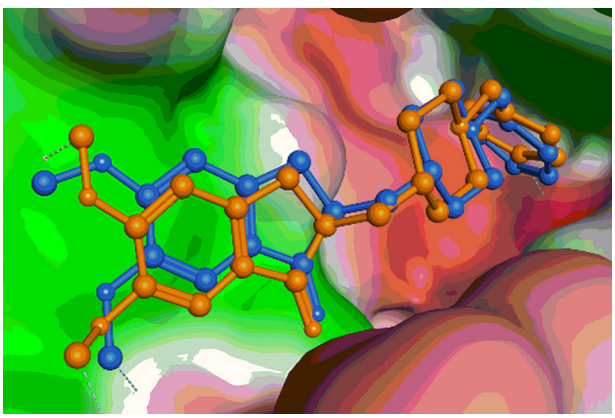

Figure 5. The overlay of native (blue) and redocked (light brown) donepezil poses in the AChE binding site.

Conclusion

We have designed and synthesized phthalimide-based compounds **7** containing the *N*-benzylpyridinium moiety as dual-binding cholinesterase inhibitors. The *in vitro* bioactivity of target compounds against AChE and BChE revealed that the 2-fluorobenzylpyridinium derivative **7d** with IC_{50} values of 0.77 and 8.71 μM was found to be the most potent compound against both enzymes. Based on the obtained results from SAR study, the type and position of substituents on the *N*-benzyl residue significantly affected the anti-cholinesterase activity. Particularly, 2-fluoro or 2-bromo substituent could improve the inhibitory activity. By comparing the inhibitory activities of the limited series of succinimide derivatives **8** with those of the corresponding phthalimide analogs **7**, it can be concluded that the aromatic part of phthalimide scaffold has important role in the inhibitory activity of the designed molecules. The docking study of the most potent compound (**7d**) into the active site of AChE showed the benzyl moiety stacks toward Trp83 and 2-fluoro group has hydrogen bonding with Glu199. Also, two aromatic-hydrophobic patches of the active site, namely CAS and PAS, are involved in the interactions.

Experimental

Chemistry

General

The commercially available reagents were purchased from Merck AG and used without further purification. Melting points were measured on a Kofler hot stage apparatus and are uncorrected. The IR spectra were taken on a Nicolet FT-IR Magna 550 spectrograph (KBr disks). ^{1}H NMR spectra were recorded on a Bruker 500 NMR instrument. The atom numbering of target compounds **7** and **8** used for NMR data interpretation is depicted in Scheme 1. The chemical shifts (δ) and coupling constant (J) are expressed in parts per million (ppm) and Hertz (Hz), respectively. Please see also the Supporting Information files for the spectra and the InChI codes of the new compounds.

*Preparation of 2-(pyridin-4-ylmethyl)isoindoline-1,3-dione **4** or 1-(pyridin-4-ylmethyl)pyrrolidine-2,5-dione **5***

Compounds **4** and **5** were prepared according to the literature [41, 42]. A mixture of phthalimide (**1**) or succinimide (**2**, 1 mmol), 4-(bromomethyl)pyridine (**3**, 1 mmol), and potassium carbonate (1.2 mmol) in DMF (8 mL) was stirred at 80°C for 8 h. After completion of reaction, the mixture was

ARCH PHARM
Archiv der Pharmazie

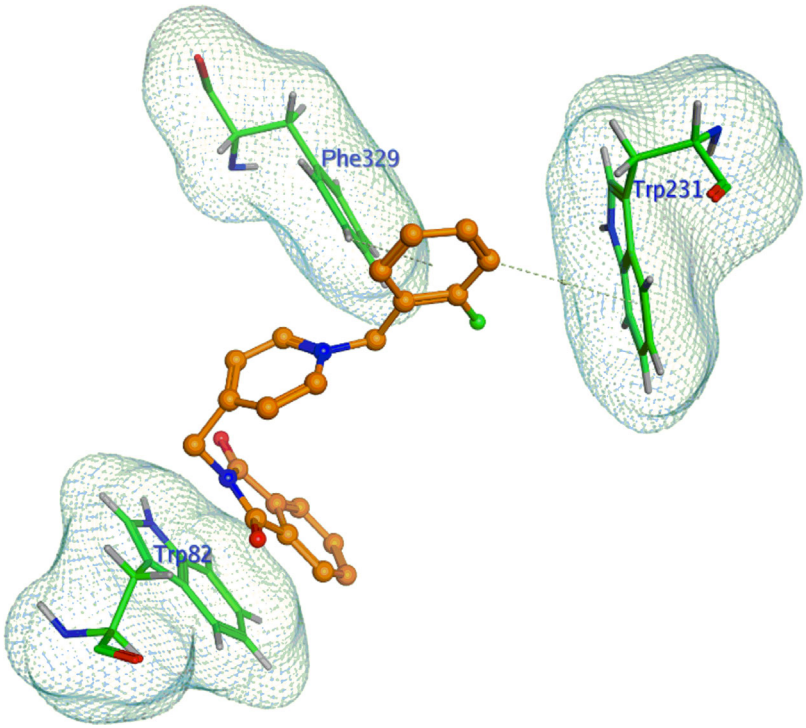

Figure 6. Molecular docking interactions pose of compound **7d** within binding pocket of BChE.

poured into crushed ice; the precipitate was filtered off and used for further reaction without purification.

*Preparation of N-benzylpyridinium salts **7** or **8***
A mixture of compound **4** or **5** (1 mmol), benzyl halide derivative **6** (1.2 mmol) in dry acetonitrile (10 mL) was heated under reflux for 7–15 h. After completion of reaction (checked by TLC), the reaction mixture was cooled to room temperature, the precipitate was filtered off, and washed with cold acetonitrile. All products were pure and did not need further purification.

*1-Benzyl-4-((1,3-dioxoisoindolin-2-yl)methyl)pyridin-1-ium bromide (**7a**)*
Yield: 75%; white solid; mp 169–170°C. IR (KBr): 3050, 2945, 1775, 1716, 1638, 1573 cm^{-1}. ^1H NMR (DMSO-d_6, 500 MHz): 5.10 (s, 2H, CH_2), 5.89 (s, 2H, CH_2), 7.42–7.57 (m, 3H, H3″, H4″, H5″), 7.56 (dd, $J = 7.5$, 1.5 Hz, 2H, H2″, H6″), 7.89–7.95 (m, 4H, H4, H5, H6, H7), 8.19 (d, $J = 6.5$ Hz, 2H, H3′, H5′), 9.21 (d, $J = 6.5$ Hz, 2H, H2′, H6′). ^{13}C NMR (DMSO-d_6, 125 MHz): 40.2, 62.6, 123.3, 126.3, 128.8, 129.2, 129.3, 131.8, 134.3, 134.6, 144.5, 156.6, 167.6. Anal. calcd. for $C_{21}H_{17}BrN_2O_2$: C, 61.63; H, 4.19; N, 6.84. Found: C, 61.80; H, 4.32; N, 6.69.

*4-((1,3-Dioxoisoindolin-2-yl)methyl)-1-(4-fluorobenzyl)-pyridin-1-ium chloride (**7b**)*
Yield: 70%; white solid; mp 234–235°C. IR (KBr): 3048, 2940, 1770, 1719, 1641, 1573 cm^{-1}. ^1H NMR (DMSO-d_6, 500 MHz): 5.09 (s, 2H, CH_2), 5.83 (s, 2H, CH_2), 7.29 (t, $J = 8.5$ Hz, 2H, H3″, H5″), 7.66 (dd, $J = 8.5$, 5.5 Hz, 2H, H2″, H6″), 7.89–7.95 (m, 4H, H4, H5, H6, H7), 8.18 (d, $J = 6.5$ Hz, 2H, H3′, H5′), 9.19 (d, $J = 6.5$ Hz, 2H, H2′, H6′). ^{13}C NMR (DMSO-d_6, 125 MHz): 40.2, 61.2, 116.1 (d, $J = 21.2$ Hz), 123.4, 126.3, 130.6, 131.4 (d, $J = 7.5$ Hz), 131.8, 134.6, 144.5, 156.7, 162.6 (d, $J = 245.0$ Hz), 167.6. Anal. calcd. for $C_{21}H_{16}ClFN_2O_2$: C, 65.89; H, 4.21; N, 7.32. Found: C, 65.74; H, 4.10; N, 7.48.

*4-((1,3-Dioxoisoindolin-2-yl)methyl)-1-(3-fluorobenzyl)-pyridin-1-ium chloride (**7c**)*
Yield: 70%; white solid; mp 236–237°C. IR (KBr): 3041, 2948, 1769, 1718, 1639, 1590 cm^{-1}. ^1H NMR (DMSO-d_6, 500 MHz): 5.09 (s, 2H, CH_2), 5.84 (s, 2H, CH_2), 7.28 (t, $J = 8.0$ Hz, 1H, H4″), 7.38 (d, $J = 8.0$ Hz, 1H, H2″), 7.46–7.53 (m, 2H, H5″, H6″), 7.89–7.95 (m, 4H, H4, H5, H6, H7), 8.19 (d, $J = 7.0$ Hz, 2H, H3′, H5′), 9.18 (d, $J = 6.5$ Hz, 2H, H2′, H6′). ^{13}C NMR (DMSO-d_6, 125 MHz): 40.2, 62.0, 115.9 (d, $J = 22.5$ Hz), 116.3 (d, $J = 20.0$ Hz), 123.4, 125.0, 126.3, 131.4 (d, $J = 7.5$ Hz), 131.8, 134.6, 136.7, 144.7, 156.8, 162.5 (d, $J = 245.0$ Hz), 167.6. Anal. calcd. for $C_{21}H_{16}ClFN_2O_2$: C, 65.89; H, 4.21; N, 7.32. Found: C, 65.97; H, 4.33; N, 7.18.

*4-((1,3-Dioxoisoindolin-2-yl)methyl)-1-(2-fluorobenzyl)-pyridin-1-ium chloride (**7d**)*
Yield: 70%; white solid; mp 175–176°C. IR (KBr): 3048, 2950, 1776, 1709, 1636, 1490 cm^{-1}. ^1H NMR (DMSO-d_6, 500 MHz): 5.02 (s, 2H, CH_2), 6.05 (s, 2H, CH_2), 7.29–7.32 (m, 2H, H5″, H6″), 7.51 (dd, $J = 13.7$, 6.5 Hz, 1H, H3″), 7.69 (t, $J = 6.5$ Hz, 1H, H4″), 7.84–7.95 (m, 4H, H4, H5, H6, H7), 8.20 (d, $J = 6.5$ Hz, 2H, H3′,

H5′), 9.21 (d, $J = 6.5$ Hz, 2H, H2′, H6′). ^{13}C NMR (DMSO-d_6, 125 MHz): 40.2, 57.2, 115.9 (d, $J = 20.3$ Hz), 121.3 (d, $J = 14.4$ Hz), 123.3, 125.2, 126.2, 131.5, 131.8, 134.6, 132.0 (d, $J = 8.1$ Hz), 144.8, 156.9, 160.4 (d, $J = 246.0$ Hz), 167.6. MS: *m/z* (%) = 382 (25), 238 (45), 147 (95), 79 (88). Anal. calcd. for $C_{21}H_{16}ClFN_2O_2$: C, 65.89; H, 4.21; N, 7.32. Found: C, 65.72; H, 4.30; N, 7.48.

*4-((1,3-Dioxoisoindolin-2-yl)methyl)-1-(2,3,5-trifluorobenzyl)-pyridin-1-ium chloride (**7e**)*
Yield: 65%; white solid; mp 223–224°C. IR (KBr): 3045, 2950, 1774, 1716, 1640, 1518 cm^{-1}. ^{1}H NMR (DMSO-d_6, 500 MHz): 5.11 (s, 2H, CH_2), 5.93 (s, 2H, CH_2), 7.61 (t, $J = 8.5$ Hz, 1H, H4″), 7.25 (ddd, $J = 10.0$, 8.5, 3.0 Hz, 1H, H6″), 7.90–7.99 (m, 4H, H4, H5, H6, H7), 8.20 (d, $J = 6.5$ Hz, 2H, H3′, H5′), 9.12 (d, $J = 6.5$ Hz, 2H, H2′, H6′). ^{13}C NMR (DMSO-d_6, 125 MHz): 40.1, 56.3, 107.5 (d, $J = 21.2$ Hz), 118.1, 120.0 (d, $J = 20.0$ Hz), 123.4, 126.2, 129.6, 131.8, 134.7, 144.9, 151.2, 156.3 (d, $J = 246.2$ Hz), 157.1, 167.7. Anal. calcd. for $C_{21}H_{14}ClF_3N_2O_2$: C, 60.23; H, 3.37; N, 6.69. Found: C, 60.36; H, 3.45; N, 6.80.

*1-(2,4-Dichlorobenzyl)-4-((1,3-dioxoisoindolin-2-yl)methyl)-pyridin-1-ium chloride (**7f**)*
Yield: 70%; white solid; mp 217–218°C. IR (KBr): 3045, 2945, 1781, 1720, 1638, 1471 cm^{-1}. ^{1}H NMR (DMSO-d_6, 500 MHz): 5.13 (s, 2H, CH_2), 5.98 (s, 2H, CH_2), 7.54 (d, $J = 8.0$ Hz, 1H, H6″), 7.58 (dd, $J = 8.0$, 2.0 Hz, 1H, H5″), 7.79 (d, $J = 2.0$ Hz, 1H, H3″), 7.90–7.96 (m, 4H, H4, H5, H6, H7), 8.19 (d, $J = 6.0$ Hz, 2H, H3′, H5′), 9.05 (d, $J = 6.0$ Hz, 2H, H2′, H6′). ^{13}C NMR (DMSO-d_6, 125 MHz): 40.2, 60.0, 123.4, 126.1, 128.2, 129.6, 130.5, 131.8, 132.9, 134.3, 134.6, 135.2, 145.0, 157.1, 167.6. Anal. calcd. for $C_{21}H_{15}Cl_3N_2O_2$: C, 58.15; H, 3.49; N, 6.46. Found: C, 58.26; H, 3.57; N, 6.58.

*1-(3,4-Dichlorobenzyl)-4-((1,3-dioxoisoindolin-2-yl)methyl)-pyridin-1-ium chloride (**7g**)*
Yield: 65%; white solid; mp 245–246°C. IR (KBr): 3049, 2950, 1770, 1711, 1641, 1465 cm^{-1}. ^{1}H NMR (DMSO-d_6, 500 MHz): 5.09 (s, 2H, CH_2), 5.85 (s, 2H, CH_2), 7.58 (d, $J = 8.0$ Hz, 1H, H6″), 7.58 (d, $J = 8.0$ Hz, 1H, H5″), 7.89–7.97 (m, 5H, H4, H5, H6, H7, H2″), 8.19 (d, $J = 6.5$ Hz, 2H, H3′, H5′), 9.19 (d, $J = 6.5$ Hz, 2H, H2′, H6′). ^{13}C NMR (DMSO-d_6, 125 MHz): 40.2, 61.2, 123.4, 126.3, 129.4, 131.4, 131.7, 131.9, 132.3, 134.7, 134.8, 135.0, 144.7, 156.9, 167.7. Anal. calcd. for $C_{21}H_{15}Cl_3N_2O_2$: C, 58.15; H, 3.49; N, 6.46. Found: C, 58.00; H, 3.28; N, 6.61.

*1-(2,6-Dichlorobenzyl)-4-((1,3-dioxoisoindolin-2-yl)methyl)-pyridin-1-ium chloride (**7h**)*
Yield: 60%; white solid; mp 221–222°C. IR (KBr): 3050, 2950, 1767, 1717, 1635, 1563 cm^{-1}. ^{1}H NMR (DMSO-d_6, 500 MHz): 5.11 (s, 2H, CH_2), 6.01 (s, 2H, CH_2), 7.60 (t, $J = 8.0$ Hz, 1H, H4″), 7.69 (d, $J = 8.0$ Hz, 2H, H3″, H5″), 7.90–7.94 (m, 4H, H4, H5, H6, H7), 8.20 (d, $J = 6.3$ Hz, 2H, H3′, H5′), 9.20 (d, $J = 6.3$ Hz, 2H, H2′, H6′). ^{13}C NMR (DMSO-d_6, 125 MHz): 40.2, 58.3, 123.3, 126.2, 129.5, 131.7, 131.8, 133.1, 134.6, 136.5, 144.5, 157.0, 167.5. Anal. calcd. for $C_{21}H_{15}Cl_3N_2O_2$: C, 58.15; H, 3.49; N, 6.46. Found: C, 58.26; H, 3.60; N, 6.55.

*1-(4-Bromobenzyl)-4-((1,3-dioxoisoindolin-2-yl)methyl)-pyridin-1-ium bromide (**7i**)*
Yield: 75%; white solid; mp 257–258°C. IR (KBr): 3048, 2950, 1770, 1719, 1640, 1571 cm^{-1}. ^{1}H NMR (DMSO-d_6, 500 MHz): 5.10 (s, 2H, CH_2), 5.88 (s, 2H, CH_2), 7.54 (d, $J = 8.3$ Hz, 2H, H2″, H6″), 7.66 (d, $J = 8.3$ Hz, 2H, H3″, H5″), 7.89–7.95 (m, 4H, H4, H5, H6, H7), 8.20 (d, $J = 6.5$ Hz, 2H, H3′, H5′), 9.21 (d, $J = 6.5$ Hz, 2H, H2′, H6′). ^{13}C NMR (DMSO-d_6, 125 MHz): 40.2, 61.8, 122.8, 123.3, 126.3, 131.1, 131.8, 132.1, 133.5, 134.6, 144.6, 156.7, 167.6. Anal. calcd. for $C_{21}H_{16}Br_2N_2O_2$: C, 51.67; H, 3.30; N, 5.74. Found: C, 51.51; H, 3.44; N, 5.86.

*1-(3-Bromobenzyl)-4-((1,3-dioxoisoindolin-2-yl)methyl)-pyridin-1-ium bromide (**7j**)*
Yield: 60%; white solid; mp 205–206°C. IR (KBr): 3056, 2945, 1761, 1706, 1638, 1572 cm^{-1}. ^{1}H NMR (DMSO-d_6, 500 MHz): 5.10 (s, 2H, CH_2), 5.88 (s, 2H, CH_2), 7.41 (t, $J = 8.0$ Hz, 1H, H5″), 7.59 (d, $J = 8.0$ Hz, 1H, H4″), 7.63 (d, $J = 8.0$ Hz, 1H, H6″), 7.88–7.95 (m, 5H, H4, H5, H6, H7, H2″), 8.20 (d, $J = 6.7$ Hz, 2H, H3′, H5′), 9.22 (d, $J = 6.7$ Hz, 2H, H2′, H6′). ^{13}C NMR (DMSO-d_6, 125 MHz): 40.2, 61.7, 122.2, 123.3, 126.3, 128.0, 131.3, 131.7, 131.8, 132.2, 134.6, 136.6, 144.6, 156.7, 167.6. Anal. calcd. for $C_{21}H_{16}Br_2N_2O_2$: C, 51.67; H, 3.30; N, 5.74. Found: C, 51.48; H, 3.18; N, 5.62.

*1-(2-Bromobenzyl)-4-((1,3-dioxoisoindolin-2-yl)methyl)-pyridin-1-ium bromide (**7k**)*
Yield: 70%; white solid; mp 158–160°C. IR (KBr): 3053, 2950, 1726, 1706, 1638, 1572 cm^{-1}. ^{1}H NMR (DMSO-d_6, 500 MHz): 5.13 (s, 2H, CH_2), 5.95 (s, 2H, CH_2), 7.33 (d, $J = 8.0$ Hz, 1H, H6″), 7.42 (t, $J = 8.0$ Hz, 1H, H4″), 7.50 (t, $J = 8.0$ Hz, 1H, H5″), 7.77 (d, $J = 8.0$ Hz, 1H, H3″), 7.90–7.96 (m, 4H, H4, H5, H6, H7), 8.21 (d, $J = 7.0$ Hz, 2H, H3′, H5′), 9.0.3 (d, $J = 7.0$ Hz, 2H, H2′, H6′). ^{13}C NMR (DMSO-d_6, 125 MHz): 40.2, 62.8, 123.4, 126.1, 128.7, 131.2, 131.5, 131.6, 131.8, 133.1, 133.4, 134.7, 145.0, 157.2, 167.6. Anal. calcd. for $C_{21}H_{16}Br_2N_2O_2$: C, 51.67; H, 3.30; N, 5.74. Found: C, 51.54; H, 3.42; N, 5.90.

*4-((1,3-Dioxoisoindolin-2-yl)methyl)-1-(4-nitrobenzyl)-pyridin-1-ium bromide (**7l**)*
Yield: 60%; white solid; mp 268–269°C. IR (KBr): 3051, 2966, 1769, 1719, 1639, 1574, 1513, 1396 cm^{-1}. ^{1}H NMR (DMSO-d_6, 500 MHz): 5.12 (s, 2H, CH_2), 6.14 (s, 2H, CH_2), 7.85–7.94 (m, 6H, H4, H5, H6, H7, H2″, H6″), 8.25–8.27 (m, 4H, H3′, H5′, H3″, H5″), 9.33 (d, $J = 6.3$ Hz, 2H, H2′, H6′). ^{13}C NMR (DMSO-d_6, 125 MHz): 40.2, 61.3, 123.3, 124.1, 126.3, 130.2, 131.8, 134.6, 141.2, 144.9, 147.8, 157.0, 167.6. Anal. calcd. for $C_{21}H_{16}BrN_3O_4$: C, 55.52; H, 3.55; N, 9.25. Found: C, 55.41; H, 3.70; N, 9.05.

*4-((1,3-Dioxoisoindolin-2-yl)methyl)-1-(2-nitrobenzyl)-pyridin-1-ium bromide (**7m**)*
Yield: 75%; white solid; mp 224–226°C. IR (KBr): 3050, 2950, 1774, 1719, 1640, 1522, 1471, 1393 cm^{-1}. ^{1}H NMR (DMSO-d_6, 500 MHz): 5.15 (s, 2H, CH_2), 6.26 (s, 2H, CH_2), 7.21 (d, $J = 7.5$ Hz, 1H, H6″), 7.74 (t, $J = 7.5$ Hz, 1H, H4″), 7.83 (t, $J = 8.0$ Hz, 1H, H5″), 7.91–7.96 (m, 4H, H4, H5, H6, H7), 8.25–8.27 (m, 3H, H3′,

H5′, H3″), 9.11 (d, $J = 5.5$ Hz, 2H, H2′, H6′). ^{13}C NMR (DMSO-d_6, 125 MHz): 402, 60.0, 123.4, 125.6, 126.1, 129.2, 130.5, 130.6, 131.8, 134.7, 134.9, 145.3, 147.6, 157.2, 167.7. Anal. calcd. for $C_{21}H_{16}BrN_3O_4$: C, 55.52; H, 3.55; N, 9.25. Found: C, 55.69; H, 3.41; N, 9.38.

*1-Benzyl-4-((2,5-dioxopyrrolidin-1-yl)methyl)pyridin-1-ium bromide (**8a**)*
Yield: 65%; white solid; mp 237–238°C. IR (KBr): 3056, 2938, 1770, 1702, 1636, 1571, 1450 cm^{-1}. ^{1}H NMR (DMSO-d_6, 500 MHz): 2.77 (s, 4H, 2CH$_2$), 4.86 (s, 2H, CH$_2$), 5.92 (s, 2H, CH$_2$), 4.41–7.43 (m, 3H, H3′, H4′, H5′), 7.58 (d, $J = 7.5$ Hz, 2H, H2′, H6′), 8.12 (d, $J = 5.0$ Hz, 2H, H3, H5), 9.27 (d, $J = 5.0$ Hz, 2H, H2, H6). ^{13}C NMR (DMSO-d_6, 125 MHz): 28.5, 40.5, 62.5, 126.1, 128.8, 129.2, 129.3, 134.3, 144.4, 156.2, 177.5. Anal. calcd. for $C_{17}H_{17}BrN_2O_2$: C, 56.52; H, 4.74; N, 7.75. Found: C, 56.65; H, 4.58; N, 7.87.

*4-((2,5-Dioxopyrrolidin-1-yl)methyl)-1-(3-fluorobenzyl)-pyridin-1-ium bromide (**8b**)*
Yield: 75%; white solid; mp 237–238°C. IR (KBr): 3050, 2927, 1760, 1698, 1638, 1588 cm^{-1}. ^{1}H NMR (DMSO-d_6, 500 MHz): 2.76 (s, 4H, 2CH$_2$), 4.86 (s, 2H, CH$_2$), 5.87 (s, 2H, CH$_2$), 7.28–7.50 (m, 4H, H2′, H3′, H5′, H6′), 8.11 (d, $J = 5.5$ Hz, 2H, H3, H5), 9.21 (d, $J = 5.5$ Hz, 2H, H2, H6). ^{13}C NMR (DMSO-d_6, 125 MHz): 28.5, 40.5, 61.9, 115.9 (d, $J = 22.5$ Hz), 116.3 (d, $J = 21.2$ Hz), 125.0, 126.2, 131.4, 136.7, 144.5, 156.4, 162.2 (d, $J = 241.2$ Hz), 177.6. Anal. calcd. for $C_{17}H_{16}BrFN_2O_2$: C, 53.84; H, 4.25; N, 7.39. Found: C, 53.71; H, 4.39; N, 7.21.

*1-(3-Bromobenzyl)-4-((2,5-dioxopyrrolidin-1-yl)methyl)-pyridin-1-ium bromide (**8c**)*
Yield: 70%; white solid; mp 208–209°C. IR (KBr): 3051, 2950, 1735, 1695, 1641, 1571 cm^{-1}. ^{1}H NMR (DMSO-d_6, 500 MHz): 2.77 (s, 4H, 2CH$_2$), 4.86 (s, 2H, CH$_2$), 5.89 (s, 2H, CH$_2$), 7.41 (t, $J = 7.7$ Hz, 1H, H5″), 7.60 (d, $J = 7.7$ Hz, 1H, H4″), 7.63 (d, $J = 7.7$ Hz, 1H, H6″), 7.89 (s, 1H, H2″), 8.11 (d, $J = 5.7$ Hz, 2H, H3, H5), 9.24 (d, $J = 5.7$ Hz, 2H, H2, H6). ^{13}C NMR (DMSO-d_6, 125 MHz): 28.5, 40.5, 61.6, 122.2, 126.2, 128.0, 131.3, 131.7, 132.2, 136.6, 144.5, 156.3, 177.5. Anal. calcd. for $C_{17}H_{16}Br_2N_2O_2$: C, 46.39; H, 3.66; N, 6.36. Found: C, 46.48; H, 3.80; N, 6.51.

Cholinesterase inhibition assay

Electric eel (*Torpedo californica*) AChE (type VI-S), BChE (E.C.3.1.1.8, from equine serum), acetylthiocholine iodide, butyrylthiocholine iodide, 5,5′-dithiobis[2-nitrobenzoic acid] (DTNB), and donepezil hydrochloride were purchased from Sigma–Aldrich (Steinheim, Germany). Compounds stock solutions were prepared by dissolving them in the absolute ethanol and then diluted in the phosphate buffer (0.1 M, pH = 8) to obtain desired assay concentrations. The AChE inhibitory activity of compounds **7** and **8** was determined by the Ellman's spectroscopic method [43, 44] using acetylthiocholine iodide as substrate in 24-well plates. The assay solutions consisted of 2 mL phosphate buffer, 65 μL DTNB, 20 μL AChE, 35 μL inhibitors which were mixed and incubated for 15 min at 25°C. The reaction was then initiated by adding 20 μL of acetylthiocholine to each well. Then, the appearance of the thiolate dianion was monitored at 412 nm in a Synergy HTX multimode plate reader. Donepezil hydrochloride was used as the positive control. The obtained data were then further analyzed by GraphPad Prism version 6 for Windows (GraphPad Software, San Diego, California, USA, www.graphpad.com) to attain IC_{50} values. The BChE inhibition assay was similarly accomplished by using butyrylthiocholine iodide as a substrate.

This research has been supported by a grant from the Research Council of Tehran University of Medical Sciences and Iran National Science Foundation (INSF).

The authors have declared no conflicts of interest.

References

[1] Alzheimer's Disease International, World Alzheimer Report **2011**, p. 1.
[2] A. Wimo, B. Winblad, L. Jönsson, *Alzheimers Dement.* **2010**, *6*, 98–103.
[3] M. S. Albert, S. T. DeKosky, D. Dickson, B. Dubois, H. H. Feldman, N. C. Fox, A. Gamst, D. M. Holtzman, W. J. Jagust, R. C. Petersen, P. J. Snyder, M. C. Carrillo, B. Thies, C. H. Phelps, *Alzheimers Dement.* **2011**, *7*, 270–279.
[4] A. Contestabile, *Behav. Brain Res.* **2011**, *221*, 334–340.
[5] L. A. Craig, N. S. Hong, R. J. McDonald, *Neurosci. Biobehav. Rev.* **2011**, *35*, 1397–1409.
[6] E. Giacobini, *Pharmacol. Res.* **2004**, *50*, 433–440.
[7] M. S. García-Ayllón, D. H. Small, J. Avila, J. Sáez-Valero, *Front. Mol. Neurosci.* **2011**, *4*, 22.
[8] A. Coin, E. Perissinotto, S. Catanzaro, M. Mosele, M. De Rui, A. Girardi, E. M. Inelmen, E. D. Toffanello, E. Manzato, G. Sergi, *Aging Clin. Exp. Res.* **2012**, *24*, 14–16.
[9] T. Darreh-Shori, H. Soininen, *Curr. Alzheimer Res.* **2010**, *7*, 67–73.
[10] M. M. Mesulam, A. Guillozet, P. Shaw, A. Levey, E. Duysen, O. Lockridge, *Neuroscience* **2002**, *110*, 627–639.
[11] I. R. Macdonald, K. Rockwood, E. Martin, S. J. Darvesh, *J. Alzheimers Dis.* **2014**, *42*, 379–384.
[12] A. Alvarez, R. Alarcon, C. Opazo, E. O. Campos, F. J. Munoz, F. H. Calderon, F. Dajas, M. K. Gentry, B. P. Doctor, F. G. De Mello, N. C. Interosa, *J. Neurosci.* **1998**, *18*, 3213–3223.
[13] M. Bartolini, C. Bertucci, V. Cavrini, V. Andrisano, *Biochem. Pharmacol.* **2003**, *65*, 407–416.
[14] D. Muñoz-Torrero, *Curr. Med. Chem.* **2008**, *15*, 2433–2455.

[15] M. del Monte-Millán, E. García-Palomero, R. Valenzuela, P. Usán, C. de Austria, P. Muñoz-Ruiz, L. Rubio, I. Dorronsoro, A. Martínez, M. Medina, *J. Mol. Neurosci*. **2006**, *30*, 85–88.
[16] J. L. Sussman, M. Harel, F. Frolow, C. Oefner, A. Goldman, L. Toker, I. Silman, *Science* **1991**, *253*, 872–879.
[17] G. Kryger, I. Silman, J. L. Sussman, *Structure* **1999**, *7*, 297–307.
[18] N. Guzior, A. Więckowska, D. Panek, B. Malawska, *Curr. Med. Chem*. **2015**, *22*, 373–404.
[19] D. M. Du, P. R. Carlier, *Curr. Pharm. Des*. **2004**, *10*, 3141–3156.
[20] M. Catto, L. Pisani, F. Leonetti, O. Nicolotti, P. Pesce, A. Stefanachi, S. Cellamare, A. Carotti, *Bioorg. Med. Chem*. **2013**, *21*, 146–152.
[21] G. Koellner, G. Kryger, C. B. Millard, I. Silman, J. L. Sussman, T. Steiner, *J. Mol. Biol*. **2000**, *296*, 713–735.
[22] A. Saxena, J. M. Fedorko, C. R. Vinayaka, R. Medhekar, Z. Radić, P. Taylor, O. Lockridge, B. P. Doctor, *Eur. J. Biochem*. **2003**, *270*, 4447–4458.
[23] H. Nadri, M. Pirali-Hamedani, M. Shekarchi, M. Abdollahi, V. Sheibani, M. Amanlou, A. Shafiee, A. Foroumadi, *Bioorg. Med. Chem*. **2010**, *18*, 6360–6366.
[24] P. Kapková, V. Alptüzün, P. Frey, E. Erciyas, U. Holzgrabe, *Bioorg. Med. Chem*. **2006**, *14*, 472–478.
[25] F. Baharloo, M. H. Moslemin, H. Nadri, A. Asadipour, M. Mahdavi, S. Emami, L. Firoozpour, R. Mohebat, A. Shafiee, A. Foroumadi, *Eur. J. Med. Chem*. **2015**, *93*, 196–201.
[26] H. Akrami, B. F. Mirjalili, M. Khoobi, H. Nadri, A. Moradi, A. Sakhteman, S. Emami, A. Foroumadi, A. Shafiee, *Eur. J. Med. Chem*. **2014**, *84*, 375–381.
[27] M. Khoobi, M. Alipour, A. Sakhteman, H. Nadri, A. Moradi, M. Ghandi, S. Emami, A. Foroumadi, A. Shafiee, *Eur. J. Med. Chem*. **2013**, *68*, 260–269.
[28] D. Alonso, I. Dorronsoro, L. Rubio, P. Munoz, E. García-Palomero, M. Del Monte, A. Bidon-Chanal, M. Orozco, F. Luque, A. Castro, *Bioorg. Med. Chem*. **2005**, *13*, 6588–6597.
[29] H. Sugimoto, Y. Iimura, Y. Yamanishi, K. Yamatsu, *J. Med. Chem*. **1995**, *38*, 4821–4829.
[30] H. M. Greenblatt, C. Guillou, D. Guénard, A. Argaman, S. Botti, B. Badet, C. Thal, I. Silman, J. L. Sussman, *J. Am. Chem. Soc*. **2004**, *126*, 15405–15411.
[31] W. Si, T. Zhang, L. Zhang, X. Mei, M. Dong, K. Zhang, J. Ning, *Bioorg. Med. Chem. Lett*. DOI: 10.1016/j.bmcl.2015.07.052
[32] A. Więckowska, K. Więckowski, M. Bajda, B. Brus, K. Sałat, P. Czerwińska, S. Gobec, B. Filipek, B. Malawska, *Bioorg. Med. Chem*. **2015**, *23*, 2445–2457.
[33] N. Guzior, M. Bajda, M. Skrok, K. Kurpiewska, K. Lewiński, B. Brus, A. Pišlar, J. Kos, S. Gobec, B. Malawska, *Eur. J. Med. Chem*. **2015**, *92*, 738–749.
[34] N. Guzior, M. Bajda, J. Rakoczy, B. Brus, S. Gobec, B. Malawska, *Bioorg. Med. Chem*. **2015**, *23*, 1629–1637.
[35] M. Saeedi, S. Ansari, M. Mahdavi, R. Sabourian, T. Akbarzadeh, A. Foroumadi, A. Shafiee, *Synth. Commun*. **2015**, *45*, 2311–2318.
[36] M. Mohammadi-Khanaposhtani, M. Mahdavi, M. Saeedi, R. Sabourian, M. Safavi, M. Khanavi, A. Foroumadi, A. Shafiee, T. Akbarzadeh, *Chem. Biol. Drug Des*. **2015**, *86*, 1425.
[37] M. Mohammadi-Khanaposhtani, M. Saeedi, N. S. Zafarghandi, M. Mahdavi, R. Sabourian, E. K. Razkenari, H. Alinezhad, M. Khanavi, A. Shafiee, A. Foroumadi, T. Akbarzadeh, *Eur. J. Med. Chem*. **2015**, *92*, 799–806.
[38] S. M. Bagheri, M. Khoobi, H. Nadri, A. Moradi, S. Emami, L. Jalili-Baleh, F. Jafarpour, F. H. Moghadam, A. Foroumadi, A. Shafiee, *Chem. Biol. Drug Des*. **2015**, *86*, 1215–1220.
[39] A. Rayatzadeh, M. Saeedi, M. Mahdavi, Z. Rezaei, R. Sabourian, M. H. Mosslemin, T. Akbarzadeh, A. Foroumadi, A. Shafiee, *Monatsh. Chem*. **2015**, *146*, 637–643.
[40] G. M. Morris, D. S. Goodsell, R. S. Halliday, R. Huey, W. E. Hart, R. K. Belew, A. J. Olson, *J. Comput. Chem*. **1998**, *19*, 1639–1662.
[41] X. Collin, J. M. Robert, G. Wielgosz, G. L. Baut, C. Bobin-Dubigeon, N. Grimaud, J. Y. Petit, *Eur. J. Med. Chem*. **2001**, *36*, 639–649.
[42] W. G. Verschueren, I. Dierynck, K. I. E. Amssoms, L. Hu, P. M. J. G. Boonants, G. M. E. Pille, F. F. D. Daeyaert, K. Hertogs, D. L. N. G. Surleraux, P. B. T. P. Wigerinck, *J. Med. Chem*. **2005**, *48*, 1930–1940.
[43] G. L. Ellman, K. D. Courtney, V. Andres, Jr., R. M. Featherstone, *Biochem. Pharmacol*. **1961**, *7*, 88–95.
[44] M. Alipour, M. Khoobi, H. Nadri, A. Sakhteman, A. Moradi, M. Ghandi, A. Foroumadi, A. Shafiee, *Arch. Pharm*. **2013**, *346*, 577–587.